

The Role of Backbone Conformation in Deltorphan II Binding: A QSAR Study of New Analogues Modified in the 5-, 6-Positions of the Address Domain

Stephen E. Schullery,^a David W. Rodgers,^a Sakambari Tripathy,^a
Don Eranda Jayamaha,^a Medha D. Sanvordekar,^a Kutralanathan Renganathan,^a
Carol Mousigian^b and Deborah L. Heyl^{a,*}

^aDepartment of Chemistry, Eastern Michigan University, Ypsilanti, MI 48197, USA

^bCollege of Pharmacy, The University of Michigan, Ann Arbor, MI 48109, USA

Received 13 February 2001; accepted 10 May 2001

Abstract—The δ selectivity of the opioid heptapeptides deltorphin I and II has been attributed to the C-terminal ‘address’ domain, the hydrophobic Val⁵–Val⁶ residues apparently playing a topographical role. We now report the synthesis, opioid binding affinities, and a QSAR study of a series of peptides in which one of the valine side chains was altered. QSAR analyses included previously published models for a binding pocket interaction and an optimum size (Schullery, S.; Mohammedshah, T.; Makhoulouf, H.; Marks, E.; Wilenkin, B.; Escobar, S.; Mousigian, C.; Heyl, D. *Bioorg. Med. Chem.* **1997**, 5, 2221), and a new approach for backbone conformational effects using Langevin dynamics simulation (PM3 semi-empirical force field) of an isolated peptide fragment containing the side chain and flanking peptide bonds. No evidence is found of binding pocket interactions or optimum size for either the position-5 or -6 side chain. Rather, δ binding is generally disfavored while μ binding is either unaffected (position-5) or favored (position-6) by larger side chains. The dynamics results provide evidence of similar ‘local’ conformation roles for the positions 5 and 6 side chains. Specifically, δ binding is favored by side chains that maximize the extension of the backbone, measured as the through-space distance between peptide fragment ends, the angle between lines connecting the α -carbon with fragment ends, or the difference between the psi and phi peptide angles. © 2001 Elsevier Science Ltd. All rights reserved.

Introduction

While opiate drugs have been used for centuries for the control of pain, the presence of toxic side effects such as respiratory depression, dysphoria, and tolerance and dependence concomitant with the prolonged administration of opioids, particularly morphine, has driven the search for a novel analgesic without these negative properties. The basis for such a search is predicated on the existence of different types of opioid receptors, designated delta, mu, and kappa,¹ where opioids interact to mediate the analgesic or antinociceptive effect. Currently, support exists for subtypes of each receptor as well; for example, δ_1 and δ_2 . These receptors are also involved in promoting addiction and tolerance, possibly through binding of more than one type of receptor at

the same time, as well as a variety of other interacting effects including behavior and mood changes, immunosuppressive effects, inflammatory responses, constipation, sedation, and the maintenance of homeostasis between electrolytes and body fluids.²

The opioid receptors belong to the rhodopsin family of G-protein coupled receptors and consist of seven transmembrane regions in the shape of alpha helices, joined by small loops; at the top are the extracellular loops (ECLs) that project into the extracellular space and at the bottom are the intracellular loops (ICLs) that extend into the cytosol. Although all three opioid receptors have been cloned, their exact three-dimensional conformations remain elusive. Various mutagenesis/chimera experiments³ as well as computer models and docking simulations with high affinity ligands⁴ have given insight into proposed interactions of the δ receptor, in particular, with opioid compounds. Some evidence supports multiple modes of binding by both

*Corresponding author. Tel.: +1-734-487-2057; fax: +1-734-487-1496; e-mail: debbie.heyhl-clegg@emich.edu

agonists and antagonists, even the lack of a requirement for overlap of important pharmacophoric elements in different peptides; details have been illustrated elsewhere.^{4,5}

Highly selective agonists and antagonists may serve as pharmacological tools to delineate the specific unequivocal role of each receptor type. It is yet to be determined whether there is a combination of receptors necessary to effect analgesia or whether the most efficacious pain relief can be attained through binding of a single receptor type. δ Agonists have emerged as promising in that they produce analgesia with a lower incidence of tolerance, dependence and gastrointestinal side effects.⁶ Recently, compounds related to the TIPP peptides with a mixed μ agonist/ δ antagonist profile have been reported to show promise as nonaddictive opioid drugs,^{7–9} since δ receptors appear to mediate the development of μ receptor-associated morphine tolerance in rodents.^{10–13}

Given the obvious pharmacological importance of δ receptors and ligands, our research has been focused on defining the stereoelectronic, structural and topographical binding requirements for one family of opioid peptides, the deltorphins, which were isolated from the skin of *Phyllomedusa bicolor* in 1989.¹⁴ The deltorphins consist of three heptapeptides that display extremely high affinities and selectivities for δ opioid receptors: deltorphin I or B (Tyr-D-Ala-Phe-Asp-Val-Val-Gly-NH₂); deltorphin II or C (Tyr-D-Ala-Phe-Glu-Val-Val-Gly-NH₂), and dermenkephalin or deltorphin A (Tyr-D-Met-Phe-His-Leu-Met-Asp-NH₂).^{2,14} Their N-terminal regions share similar amino acid sequences to the dermorphins, while their C-terminal tails differ markedly from the latter μ -selective family. These peptides, especially deltorphin II, display a high affinity for binding to the δ receptor, and they show a tremendous selectivity in binding as well, demonstrating 3000 times more affinity for δ receptors versus μ receptors.¹⁴ The reasons for this extraordinary selectivity have been the subject of much consideration, but most ideas center around interactions with the amino acids in the C-terminal 'address' domain,^{15–18} since the N-terminal 'message' domain alone has already been proven to be specific to μ receptor binding.¹⁹

The C-terminal tail of the deltorphins has been shown to assume an extended, rather than helix-like, conformation where the fifth, sixth and seventh residues fold underneath the first through fourth residues, which may favor some sort of hydrogen-bonded 'head-to-tail' pseudo-cyclization.^{20–22} The high flexibility of the deltorphins has led to an interpretation of some data as implying a number of different β -turns based on the appearance of a multitude of low-energy conformers at equilibrium.^{23–25} The hydrophobic nature of the C-terminal tail of the deltorphins appears important for δ receptor selectivity,^{26,27} whether for direct hydrophobic contact with the receptor or for stabilizing the preferred conformation for receptor interaction. Quantitative 2D-NMR and energy calculation studies suggests that the C-terminal domain influences the backbone conformation

of the N-terminal tetrapeptide,^{28,29} and some studies have implied a lesser role for Val⁶ than Val⁵ in δ receptor binding.²⁷

Hundreds of deltorphin analogues have been synthesized in the quest for structure–activity relationships (see refs 30 and 31 for reviews). They include compounds in which the N-terminus and/or C-terminus have been extended, amino acids have been deleted, amide bonds have been replaced by isosteres, the peptide has been glycosylated and/or phosphorylated (to improve the non-diffusive blood–brain barrier permeability), conformational restrictions have been employed, and native amino acids have been substituted by other conventional or novel amino acids. Our research has utilized the latter approach, specifically, QSAR studies of deltorphin I and II side-chain analogues of the message-domain residue 3 and the address-domain residue 4,³² as well ω -amino acid backbone analogues of the address-domain residues 5 and 6.³³ QSAR suggested that the residue-3 side chain binds to similar, hydrophobic pockets on the δ and μ receptors, whereas the residue-4 side chain interacts electrostatically with a positive-charged binding pocket, but only on the δ receptor. Presumed steric clash between the residue-4 side chain and the μ receptor provides a possible mechanism of δ selectivity.³² In contrast to the side chain studies, the ω -amino acids used in the residues 5 and 6 study had no side-chains (nor α -carbon DL-stereo centers), so the testable model envisioned binding of the *entire* C-terminal tripeptide into a hydrophobic pocket or cleft on the receptor.³³ A binding pocket interaction was hypothesized to be relatively compatible with modifications that roughly maintain the overall size, shape and hydrophobicity of the tail. The alternative hypothesis, conformational stabilization, predicted that binding would be more sensitive to changes in the tail structure, particularly removal of the L stereo restraint. Such sensitivity was indeed observed; no QSAR support for a whole C-terminus binding pocket was found with either the δ or μ receptors, and the conformation stabilization theory was accepted.

However, the conformation stabilization hypothesis was accepted by default, and the detailed roles, if any, of the individual Val side-chain moieties were not addressed. Specifically, the possibility remained for binding pockets of the individual Val side chains on the receptor. Further, the data did not discriminate between two possible conformational mechanisms: (1) an interaction between the Val side chains and some remote segment(s) of the deltorphin molecule, and (2) a more local effect of the Val side chains on the backbone geometry (e.g., adjacent ϕ – ψ angles). To address those issues, we now report a study of the side chains of residues 5 and 6.

Nineteen new Val⁵ analogues and 17 new Val⁶ analogues are reported in which the Val residue is replaced by an L- α -amino acid differing only in the nature of its side chain. All replacement side chains are non-ionizable. The δ and μ receptor binding affinities of the analogues are subjected to three QSAR analyses: (1) the hydrophobic side chain binding-pocket model, (2) a

quadratic, optimum-value model, consistent with either binding-pocket or conformational roles, and (3) a new local geometry model that tests directly for a conformational effect in terms of local backbone geometry around the substituted α -carbon.

QSAR Strategies

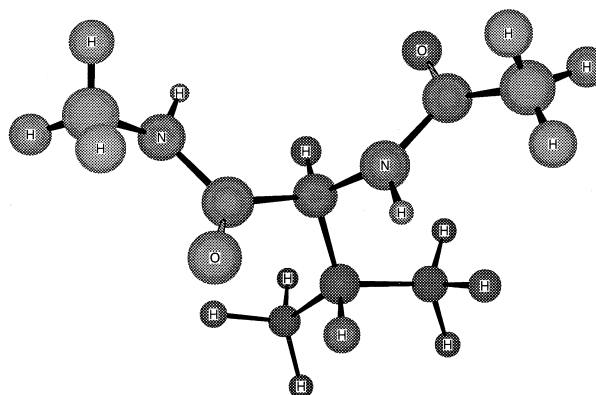
For all QSAR analyses, binding affinity is analyzed in terms of the logarithm of binding enhancement factors, $\log E_\delta$ and $\log E_\mu$. The enhancement factors E_δ and E_μ are defined as the ratios of the native $K_{i\delta}$ or $K_{i\mu}$ to the analogue $K_{i\delta}$ or $K_{i\mu}$, respectively. This normalization allows direct comparison of data from different laboratories, from which K_i values of the same compound can differ by two orders of magnitude.³¹ Use of the logarithm function provides a variable that is more likely to depend linearly on energy or entropy, and that conveniently gathers and distributes data spanning orders of magnitude. So defined, positive values of $\log E$ correspond to binding stronger than that of the native deltorphin.

Three types of QSAR models are tested. First, the potential-well binding model treats the ligand-binding pocket interaction as a competition between combined hydrophobic and van der Waals attractions and steric repulsion, and has been described in detail.³² Briefly, the octanol–water partition coefficient ($\log P$) and the polarizability are used as the hydrophobic and van der Waals attraction terms, respectively, along with a steric repulsion term based on van der Waals dimensions described below. Multiple regression is performed on $\log E$ as a function of $\log P$, polarizability and the steric factor. A statistically significant relationship ($p < 0.05$) for the overall F statistic and for the coefficient of each predictor variable, as well as appropriate coefficient signs—positive for $\log P$ and polarizability, and negative for the steric factor—are required for the model to be supported. This model has been successfully applied to the side chains of residues 3 and 4.³²

A second QSAR model assumes the existence of an optimum value of a variable that can be detected by regressing binding enhancement on both a linear and square term in that variable. If binding goes through a maximum over the tested range of the variable, then the linear term will have a positive coefficient and the square term a negative coefficient. The predicted optimum value can be calculated by equating the derivative of the regression equation to zero. A positive result might reflect either a receptor binding-pocket interaction or an intramolecular conformation-stabilizing interaction. This method has been used to infer the optimum length of the position-3 side chain,³² and is used in the present study to test the following side chain dimensions for the existence of an optimum value: volume, area, width, thickness, length, and normal (defined below).

The third QSAR model assumes that the side chain serves a conformational role by inducing a bias in the

local backbone geometry. For this model, a peptide fragment consisting of an α -carbon with the side chain under study and the two flanking peptide bonds ‘capped’ with methyl groups is utilized. For example, the Val peptide fragment is pictured.



Four backbone-geometry variables are simulated: the phi and psi peptide bond angles, the backbone length of the segment defined by the through-space distance between the capping methyl carbons, and the backbone angle defined by lines connecting the alpha-carbon to the terminal, capping methyl carbons. The evolution of these variables in time is simulated using the Langevin variation on molecular dynamics,³⁴ along with the PM3 semi-empirical quantum force field.³⁴ We assume that the Langevin method, which models the random thermal buffeting by liquid solvent molecules of specified viscosity and temperature on a solute molecule of specified frictional coefficient, should offer some additional realism over the simple molecular dynamics simulation of an isolated (in-vacuum) molecule.

Results

Receptor binding

Table 1 presents the binding data (along with experimental purity, column retention time, and molecular weight) for each analogue studied. Both μ and δ binding affinity data are presented, along with the logarithms of the binding enhancement factors ($\log E$) used in the QSAR analyses. The μ binding affinities for the position 5 analogues contain eight cases for which the normal limits of the binding assay were exceeded, and $K_{i\mu}$ is reported as percent displacement at the 10 μ M limit. A measure of selectivity is provided as the ratio of μ to δ binding affinities. Binding to κ -receptors was negligible ($K_i > 10,000$ nM) for all compounds, so those data are not presented. Data for the native deltorphin II and data from another laboratory²⁷ for the Ala⁵ and Ala⁶ analogues incorporated into the present analysis are also shown. Inspection of the binding data in Table 1 reveals that all of the modifications except Cha⁶ degrade δ receptor binding, whereas four of the residue 5 modifications and five of the residue 6 modifications improve μ receptor binding.

Calculated molecular properties

The calculated QSAR properties of the isolated side chains and peptide fragments are presented in Tables 2 and 3, respectively. SPSS[®] box plot analysis revealed two extreme outliers among the psi values, and one extreme outlier among the backbone length and angle data. Psi is exceptionally low for Bip and exceptionally high for Phg. The backbone length and angle are exceptionally large for the Phg fragment. Bip is unique in having two ring systems attached to the β -carbon, and Phg is unique in having the β -carbon as part of an aromatic ring. A second 500-ps dynamics run replicated phi–psi angles of Phg to within 2°. To eliminate the possibility of undue influence, the psi data for Bip and Phg, and backbone length and angle data for Phg were omitted from further analysis. To obtain an estimate of

how reliable averages from 500 ps Langevin dynamics runs are, six consecutive 500 ps runs were made using the Valine peptide fragment. The standard deviations observed were 3.6 and 2.2° for phi and psi, respectively. Although not as precise as desired, this level of reproducibility was judged usable by comparison with the sample ranges of 18 and 19° for phi and psi, respectively.

QSAR: bivariate correlations

The correlation coefficients (Pearson's product-moment r) of each QSAR variable with both δ and μ binding ($\log E_\delta$ or $\log E_\mu$) are shown in Table 4, with separate panels for the isolated side chains and peptide fragments. Correlations significant at the $p \leq 0.05$ and ≤ 0.01 level are noted with one or two asterisks, respec-

Table 1. Opioid receptor binding affinities of (X⁵) and (X⁶) Deltorhin II analogues^a

Analogue	Purity (%) ^b	HPLC-RT ^c	M_r	$K_{i\delta}$ (nM) ^d DPDPE	$\log E_\delta$	$K_{i\mu}$ (nM) ^d DAMGO	$\log E_\mu$	$K_{i\mu}/K_{i\delta}$
Val ^{5,6}	—	—	—	2.69±0.26	0	1310±130	0	487
Abu ⁵	100	14.1	768.4	9.71±1.07	−0.557	3440±426	−0.419	354
Ala ^{5e}	—	—	—	1.6	−0.472	200	0.32	125
Bip ⁵	95	18.8	906.4	14.7±4.01	−0.738	38.2%	−0.9	> 680
Cha ⁵	98	17.6	836.1	5.04±1.05	−0.273	579±76.5	0.355	115
Dip ⁵	98	17.8	906.7	19.4±0.752	−0.858	48.8%	−0.9	~ 515
F ₅ Phe ⁵	100	17.4	920.8	68.3±16.7	−1.405	37.8%	−0.9	> 146
Hfe ⁵	95	16.0	845.1	19.1±9.66	−0.851	7710±983	−0.77	404
Ile ⁵	99	14.5	797.1	15.1±1.08	−0.749	3520±504	−0.43	233
Leu ⁵	98	14.3	797.1	2.89±0.562	−0.0311	2760±397	−0.324	956
Met ⁵	95	15.6	815.6	15.1±1.17	−0.749	3640±961	−0.444	241
1Nal ⁵	95	18.0	880.7	10.4±0.972	−0.587	1070±74.4	0.0871	103
2Nal ⁵	95	17.5	880.7	12.3±3.29	−0.66	49.1±11.1	1.426	3.99
Nle ⁵	100	15.1	797.1	3.68±0.302	−0.136	1570±377	−0.0786	427
Nva ⁵	96	15.2	783.1	5.63±0.723	−0.321	37.8%	−0.9	> 1780
pCF ₃ Phe ⁵	100	18.0	898.7	87.3±9.87	−1.511	1670±102	−0.106	19.1
Phe ⁵	95	16.5	831.1	12.1±5.95	−0.653	7680±470	−0.768	635
Phg ⁵	95	16.0	817.0	8.74±1.55	−0.512	42.4%	−0.9	> 1140
<i>t</i> BuAla ⁵	99	16.3	811.0	27.1±8.34	−1.003	29.9%	−0.9	> 369
Tle ⁵	98	16.7	797.8	21.0±6.73	−0.892	39.3%	−0.9	> 476
TyrOMe ⁵	100	16.0	860.8	14.9±0.657	−0.743	2440±283	−0.27	164
Abu ⁶	100	12.8	768.4	4.40±0.268	−0.214	1060±94.4	0.092	241
Ala ^{6e}	—	—	—	1.07	−0.297	582	−0.144	542
Bip ⁶	95	19.4	906.4	14.6±1.51	−0.735	542±21.3	0.383	37.1
Cha ⁶	98	17.3	836.1	2.17±0.059	0.0933	587±21.7	0.349	271
F ₅ Phe ⁶	95	17.8	920.8	38.5±3.65	−1.156	3030±277	−0.364	78.7
Hfe ⁶	95	16.9	845.1	17.8±1.07	−0.821	1930±288	−0.168	108
Ile ⁶	97	15.0	797.1	12.1±2.09	−0.653	3330±640	−0.405	275
Leu ⁶	95	14.8	797.1	12.1±2.16	−1.095	3330±698	−0.718	275
1Nal ⁶	95	18.2	880.7	15.4±1.58	−0.758	363±50.6	0.557	23.6
2Nal ⁶	98	18.7	880.7	48.1±4.69	−1.252	1100±20.1	0.077	22.9
Nle ⁶	99	15.1	797.1	19.7±2.65	−0.865	5430±1410	−0.617	276
Nva ⁶	95	14.2	783.1	22.9±3.08	−0.93	2990±581	−0.359	131
pCF ₃ Phe ⁶	95	18.4	898.7	75.9±5.10	−1.45	1680±180	−0.109	22.1
Phe ⁶	95	16.4	831.1	25.1±2.91	−0.97	1570±249	−0.0786	62.5
Phg ⁶	90	16.0	817.0	12.7±0.737	−0.674	4720±171	−0.577	372
<i>T</i> BuAla ⁶	95	15.6	811.0	68.9±4.24	−1.408	49.9%	−0.88	145
Tle ⁶	100	16.5	797.8	114±21.8	−1.627	5210±865	−0.599	45.7
TyrOMe ⁶	100	15.8	860.6	53.2±5.03	−1.296	1940±371	−0.171	36.5

^aAbbreviations: Analogue identities and binding enhancement factors ($\log E$) are described in the text. M_r , molecular weight obtained by electrospray mass spectrometry.

^bPurity of final product peptide as assessed by RP-HPLC peak integration at 280 or 230 nm (whichever is lower), rounded to the nearest percent.

^cHPLC retention time in min on a Phenomenex C-18 column (0.46×25 cm); gradient of 0–66% organic component in 22 min; flow rate of 1 mL/min. Solvent system was 0.1% TFA in water, 0.1% TFA in acetonitrile. Solvent front breakthrough at 2.5 min.

^dAverage values from two to four assays performed in triplicate, \pm standard error of mean. Where the K_i was greater than 10 μ M (no substantial binding), percent displacements at the 10 μ M limit are given.

^eSynthesized in another laboratory.²⁷

Table 2. Calculated properties of isolated side chains

Side chain	log P	Polarizability (Å ³)	Volume (Å ³)	Area (Å ²)	Steric factor (Å ⁴)	Width (Å)	Thickness (Å)	Length (Å)	Normal (Å)	Ovality	β Crowding
1Nal	3.52	19.54	148.66	172.58	9480	5.71	1.82	7.2	6.27	2.057	1
2Nal	3.52	19.54	148.61	173.06	9533	5.34	1.81	8.03	7.63	2.075	1
Abu	1.3	4.44	46.13	69.67	1545	2.06	1.92	2.33	2.19	1.405	1
Ala	1.09	2.61	28.87	47.6	720	1.61	1.55	1.74	1.11	1.142	0
Bip	4.2	21.93	176.65	203.5	13185	4.36	1.81	10.21	12.62	2.389	1
Cha	2.71	12.85	119.36	149	7066	4.35	2.86	5.98	2.28	2.052	1
Dip	4.13	21.93	177.98	209.2	13933	4.35	3.83	8.83	5.43	2.556	2
F ₅ Phe	3.21	11.81	115.34	145	6692	6.18	1.81	5.12	5.65	2.026	1
Hfe	2.91	14.1	120.48	149	7070	4.76	1.81	7.35	10.09	2.016	1.5
Ile	2.09	8.11	80.09	111.1	3930	3.1	2.85	5.2	4.17	1.891	2.5
Leu	2.02	8.11	79.93	109.9	3846	4.36	2.71	3.97	3.51	1.838	2
Met	0.8	9.28	82.16	112	3978	3.19	2.95	5.33	4.3	1.839	1.5
Nle	2.09	8.11	80.12	111.1	3930	3.1	2.85	5.2	4.17	1.889	1.5
Nva	1.69	6.28	83	89.5	2551	2.18	1.8	4.37	3.51	1.598	1.5
pCF ₃ Phe	3.4	13.83	128.3	160.2	8167	5.5	2.24	6.16	5.94	2.210	1
Phe	2.51	12.27	103.63	128.6	5267	4.34	1.81	5.85	5.42	1.749	1
Phg	2.05	10.43	86.77	107.61	3686	4.33	1	5.00	3.9	1.463	1
<i>t</i> -BuAla	2.46	9.95	96.53	129.6	5344	3.52	3.16	3.53	3.5	2.064	2.5
Tle	2.02	8.11	79.9	109.9	3846	3.81	2.71	4.37	3.51	1.839	3
TyrOMe	2.26	14.74	127.99	159.5	8093	4.58	1.86	8.04	7.6	2.188	1
Val	1.69	6.28	62.98	89.5	2551	2.18	1.8	4.37	3.51	1.599	2

Table 3. Time-average properties of peptide fragments determined by Langevin dynamics

Side chain	Mean phi (°)	Mean psi (°)	Mean length (Å)	Mean angle (°)
1Nal	−96.8	130.8	6.53	115.92
2Nal	−102.1	118.3	6.51	115.27
Abu	−104.4	129.7	6.57	117.09
Ala	−99.7	132.7	6.56	117.02
Bip	−99.2	102.7	6.40	112.62
Cha	−100.1	129.7	6.55	116.37
Dip	−98.4	124.2	6.42	112.90
F ₅ Phe	−97.2	130.2	6.48	114.55
Hfe	−96.4	137.2	6.56	116.77
Ile	−97.9	136.7	6.59	117.67
Leu	−99.7	131.7	6.55	116.64
Met	−108.3	131.9	6.56	119.02
Nle	−100.8	136.2	6.52	115.38
Nva	−104.1	131.9	6.59	117.76
pCF ₃ Phe	−94.4	120.8	6.36	110.99
Phe	−99.4	133.4	6.54	116.31
Phg	−111.0	152.0	6.82	125.53
<i>t</i> -BuAla	−91.5	132.1	6.47	114.00
Tle	−92.8	128.1	6.42	112.69
TyrOMe	−100.7	129.1	6.54	116.07
Val	−102.8	135.9	6.60	118.13

tively, and those smaller than 0.30 (accounting for less than 9% of the variance) are omitted. Four trends are noteworthy: (1) An inverse relationship (i.e., negative correlation) exists between δ binding and side chain size of both residues 5 and 6. However, of the several size-related variables having negative correlations with δ binding, only ovality and width attain statistical significance. (2) A direct relationship (i.e., positive correlation) exists between μ binding and side chain size of residue 6, with five of the correlations attaining statistical significance. The corresponding correlations at residue 5 are negligible. (3) An inverse relationship exists between μ binding and β crowding, although statistical significance is obtained only at residue 6. (4) A

Table 4. Correlations between δ or μ binding and QSAR variables^a

Variable	Residue 5 ^b		Residue 6 ^c	
	log E _{δ}	μ rank	log E _{δ}	Log E _{μ}
Isolated side chains				
Log P	−0.43	—	−0.33	0.44
Polarizability	−0.34	—	—	0.53*
Volume	−0.39	—	—	0.47*
Area	−0.42	—	−0.36	0.42
Steric factor	−0.39	—	−0.30	0.51*
Ovality	−0.44*	—	−0.46*	—
Width	−0.53*	—	−0.49*	—
Thickness	—	—	—	−0.37
Length	—	—	—	0.47*
Normal	—	—	−0.30	0.36
β-crowding	—	−0.39	−0.33	−0.55*
Peptide fragments				
Mean phi	−0.48*	—	−0.50*	—
Mean psi	0.43	—	0.42	—
Mean (psi + phi)	—	−0.35	—	−0.42
Mean (psi − phi)	0.63**	—	0.66**	—
Mean length	0.64**	0.32	0.60**	—
Mean angle	0.61**	—	0.63**	—

*Correlation significant at the 0.05 level (two-tailed). **Correlation significant at the 0.01 level (two-tailed).

^aCorrelations <0.030 not shown.

^b $n=21$ except for psi variables, from which extreme outliers Bip and Phg were removed leaving $n=19$, and length and angle variables, from which extreme outlier Phg was removed leaving $n=20$.

^c $n=19$ except for psi variable, $n=17$, and length and angle variables, $n=18$.

direct relationship exists between δ binding and the extension of the peptide backbone at both residues 5 and 6, as indicated by positive correlations with backbone length, backbone angle, and the combination variable (psi − phi). The latter is consistent with the weaker correlations of the individual psi and phi angles. The linear relationships between δ binding and (psi − phi) for the position 5 and position 6 analogues are shown in Figures 1 and 2, respectively. Of course, the psi and phi angles are not independent of the backbone length and

angle; in the present data set, the mean length and angle correlate with psi and phi at 0.63 and -0.62 , respectively, and with (psi–phi) at 0.89. The linear relationship between backbone length and (psi–phi) is illustrated in Figure 3.

The relatively weak relationship between δ binding and side-chain size, compared to the stronger relationship between δ binding and backbone extension, suggests that backbone extension is the more fundamentally important variable. Further, each of the three backbone

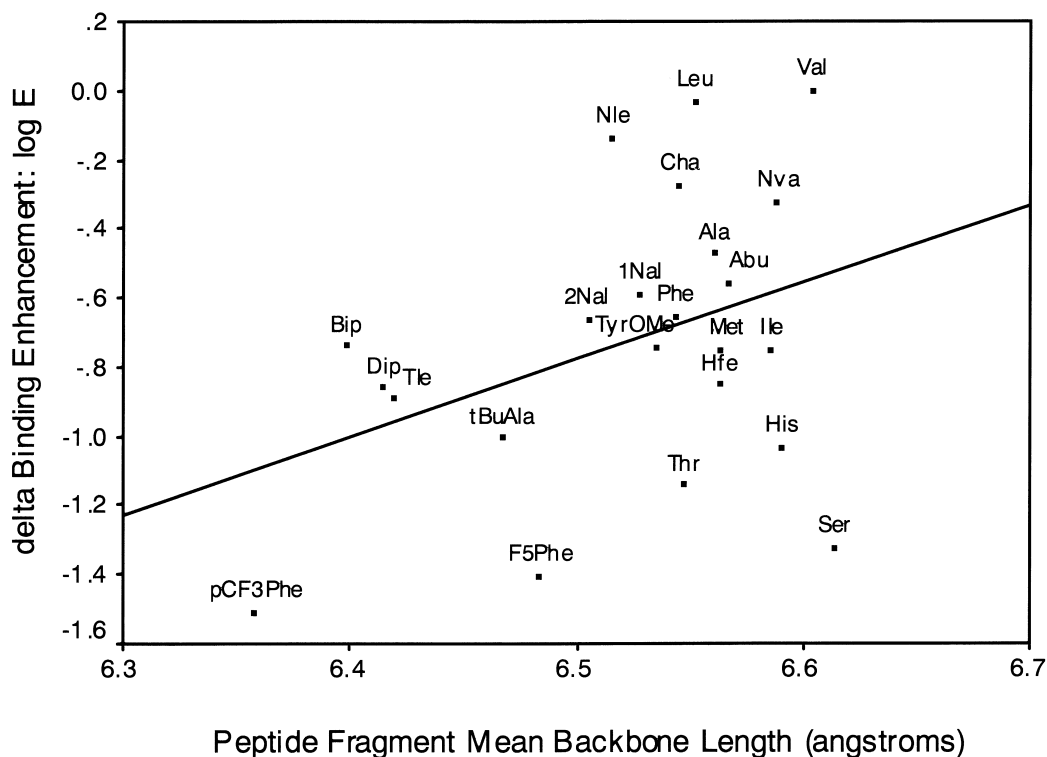


Figure 1. Plot of $\log E_{\delta}$ of the residue 5 analogues versus the mean backbone length of corresponding peptide fragment, as determined by Langevin dynamics simulation. Least squares best-fit line is shown.

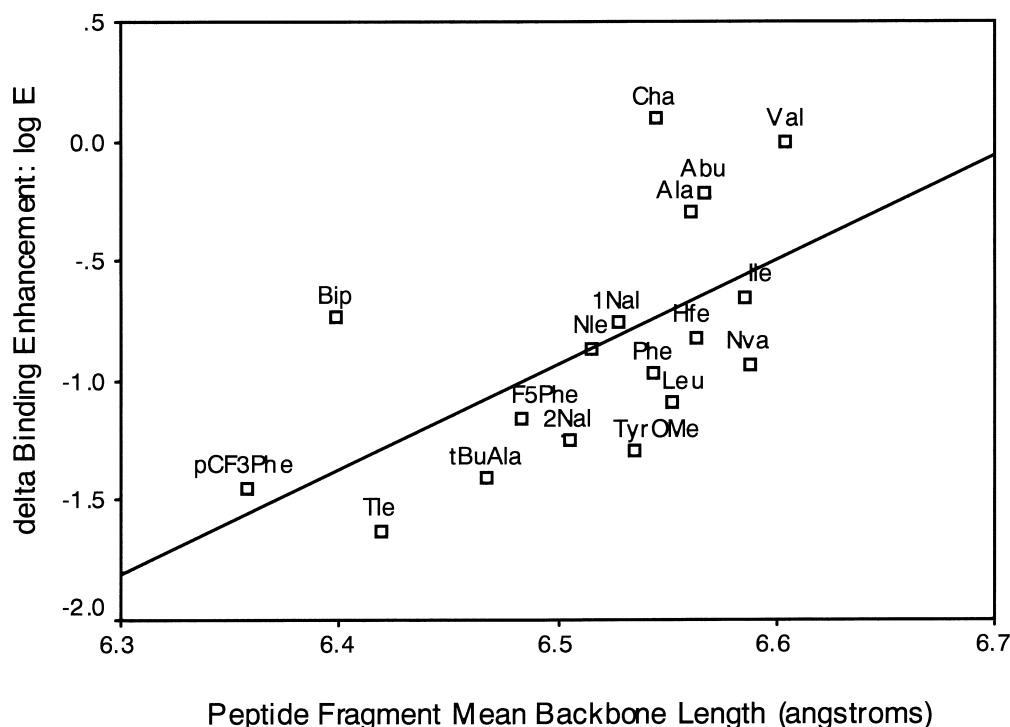


Figure 2. Plot of $\log E_{\delta}$ of the residue 6 analogues versus the mean backbone length of corresponding peptide fragment, as determined by Langevin dynamics simulation. Least squares best-fit line is shown.

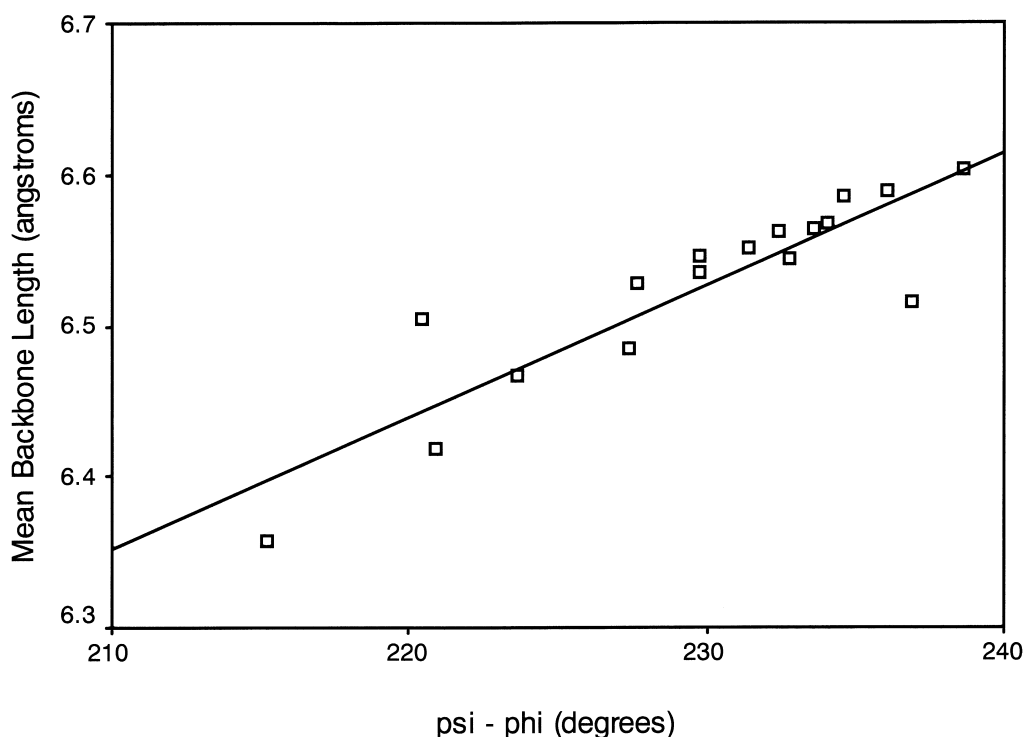


Figure 3. Plot of the peptide fragment mean backbone length versus the difference between the mean psi and phi angles, all data as determined by Langevin dynamics simulation. Least squares best-fit line is shown.

extension variables (length, angle, psi–phi) correlates significantly, and inversely, with seven of the 10 side chain size-related variables. Such compression of the other bond angles on the α -carbon by large side chains would be expected on simple steric grounds. However, the similarly reasonable expectation that β crowding in the side chain should be particularly effective at compressing the other α -carbon bond angles is not met; β crowding correlates with none of the backbone extension variables.

The role(s) of Val⁵ and Val⁶ in the δ/μ selectivity of the native deltorphin II can be analyzed in terms of variables that have differential effects on δ versus μ binding. The suitability of the Val side chain for maintaining δ selectivity is evident in three respects: First, the relatively large extension that Val produces in the peptide backbone (e.g., see length and angle data in Table 3) promotes δ binding, while not affecting μ binding. Second, Val is small enough to neither weaken δ binding nor strengthen μ binding (at position 6). Finally, the relatively high β crowding of Val weakens μ binding, particularly at position 6, with little effect on δ binding.

QSAR: multiple regression

Multiple regression analyses were performed for the position 5 analogues using $\log E_{\delta}$ and the rank-ordered μ binding affinity as dependent variables, and for the position 6 analogues using $\log E_{\delta}$ and $\log E_{\mu}$ as dependent variables. Tests of the binding pocket model used the following combinations of independent variables: $\log P$, polarizability, and steric factor; $\log P$ and steric factor; polarizability and steric factor. Tests of the

optimum-size model used as independent variables a linear and a square term of the following: width, thickness, length, normal, volume, and area. Regression data are not shown because in no case was a significant relationship observed. That is, neither the binding pocket model nor the optimum size model could be fit to these data.

Exploratory stepwise regression of $\log E_{\delta}$ and $\log E_{\mu}$ versus the entire set of 10 size-related variables, β crowding, psi, phi, (psi–phi), and (psi + phi) uncovered only one unanticipated multivariate relationship. For the position 6 analogues, μ binding is both positively related to polarizability and negatively related to β crowding, with a multiple R of 0.694 ($p=0.005$) and standardized regression coefficients of 0.429 ($p=0.034$) and -0.461 ($p=0.024$) for polarizability and β -crowding, respectively. Further study indicated that the other size variables gave similar relationships when substituted for polarizability, although only the length and steric factor variables achieved $p \leq 0.05$ significance. These findings are consistent with the bivariate correlations of the same variables (Table 4), and show that the size and β crowding variables provide independent explanatory power. That they work in opposite directions is somewhat surprising, as one might expect size to cause β crowding. In fact, β crowding correlates with only one of the 10 side-chain size-related variables, thickness ($r=0.62$). Of course, the importance of these μ binding results is limited because, although a few of the analogues improved on the μ affinity of the native compound, none approached the tight binding characteristic of the δ interaction. Thus, extrapolations into a tight μ binding regime would be speculative.

Finally, we note that our results present two surprises regarding δ binding. First, our data do not support the notion that residue 5 is more important than residue 6 for δ receptor interaction.^{27,33} The average decrement in δ binding is larger for the position 6 series (log $E_\delta = -1.05$) than for the position 5 series (log $E_\delta = -0.76$). Also, δ binding is only marginally more sensitive to changes in side-chain size, and marginally less sensitive to changes in β crowding and backbone extension, at position 5 than position 6. Second, the common assumption that hydrophobicity at positions 5 and 6 is important for δ binding^{26,27} is not supported for the range of log P values captured by the present data set. There was no bivariate or multivariate relationship connecting log P with δ (or μ) binding. Rather, at least within a group containing only hydrocarbon or other non-hydrophilic side chains, the dependence of log P on molecular size asserts itself such that log P behaves as just another size-surrogate variable.

Conclusions

Smaller side chains, such as Val at residues 5 and 6 of the native deltorphin, permit and/or promote greater extension of the backbone at those segments, which, in turn, promotes tighter δ binding. Smaller side chains also promote δ selectivity by disfavoring μ binding (at residue 6). The high β crowding of the native Val side chains further promote δ selectivity by disfavoring μ binding, particularly at residue 6. These findings, together with the absence of binding pocket interactions by either the side chains of residues 5 and 6 (present study) or the C-terminal tripeptide,³³ suggests that backbone extension at residues 5 and 6 serves to stabilize an optimal binding conformation of the pharmacophore portion of the deltorphin molecule.

Experimental

Peptide synthesis

The following amino acid replacements were made independently at residues 5 and 6: α -aminobutyric acid (Abu), β , β -biphenylalanine (Bip), β -cyclohexylalanine (Cha), *para*-phenylphenylalanine or diphenylalanine (Dip), pentafluorophenylalanine (F_5 Phe), homophenylalanine (Hfe), isoleucine (Ile), leucine (Leu), methionine (Met), 3-(1-naphthyl)alanine (1Nal), 3-(2-naphthyl)alanine (2Nal), norleucine (Nle), norvaline (Nva), *para*-trifluoromethylphenylalanine (pCF_3 Phe), phenylalanine (Phe), phenylglycine (Phg), *tert*-butylalanine (*t*BuAla), *tert*-butylglycine or *tert*-leucine (Tle), and *para*-methoxyphenylalanine or tyrosine methyl ether (TyrOMe).

All of the protected or novel amino acids, coupling agents and resins were purchased from Bachem (King of Prussia, PA). Solvents and deprotecting agents were obtained from Fisher Scientific (Itasca, IL) and Aldrich Chemical Co. (Milwaukee, WI). Radioligands were purchased from New England Nuclear (Boston, MA),

Multiple Peptide Systems (San Diego, CA) and Amer-sham (Piscataway, NJ), and frozen guinea pig brains were obtained from Rockland, Inc. (Gilbertsville, PA). The peptides were prepared on a St. John's Associates manual shaker using standard solid-phase techniques for *N*- α -*t*-butyloxycarbonyl (Boc) protected amino acids on *p*-methylbenzhydrylamine (MBHA) resin (0.6–1.1 mmol/g). The side chain of Tyr was protected as the 2,6-dichlorocarbobenzyloxy derivative and Glu, as the benzyl ester. The deprotection solution for the N-terminal amine was 30% trifluoroacetic acid (TFA) in dichloromethane (DCM). Dicyclohexylcarbodiimide (DCC) or diisopropylcarbodiimide (DIC) and *N*-hydroxybenzotriazole (HOBt) were used as coupling agents. The protocol for peptide synthesis in each cycle was as described previously.³² Simultaneous deprotection and cleavage from the resin were accomplished by treatment with 90% anhyd HF (Immunodynamics apparatus) and 10% anisole scavenger (10 mL of HF and 1 mL of anisole per gram of resin) at 0°C for 1 h. After evaporation of the HF, the peptide resin was washed with diethyl ether and the peptide was extracted with 70% acetonitrile/30% water (with 0.1% TFA), concentrated under reduced pressure, diluted with water, and lyophilized. Crude peptides were purified to homogeneity by preparative reversed-phase high performance liquid chromatography (RP-HPLC) on a Waters instrument with a Vydac C18 column (2.2×25.0 cm, 10 mL/min). A linear gradient of water (0.1% TFA) to 50% acetonitrile (0.1% TFA)/water (0.1% TFA) over 2 h was employed, followed by lyophilization. Attaining the desired solubility, in any of several mobile phases tested, was difficult for some of the hydrophobic residue 6 analogues, including Phg⁶ discussed below.

Peptide analysis

Peptide purity was assessed by analytical RP-HPLC using the same solvent system and a gradient of 0–66% organic component over 22 min (Phenomenex Jupiter column, 0.46×25 cm, 1.0 mL/min). Peaks were monitored at 214, 230, 254, and 280 nm. All compounds except one (Phg⁶, 90%) were at least 95% pure as analyzed by peak integration. Given the inherent variability in binding assay data and the desirability to include the maximum possible number of analogues for analysis, the Phg⁶ compound was retained for the QSAR study. However, coincidentally, the Phg peptide fragment generated some extreme-outlier *calculated* dynamics properties, necessitating that it be dropped from some of the QSAR analyses. Proton nuclear magnetic resonance (¹H NMR) spectra were obtained on a Bruker spectrometer at 250 MHz. Samples (approx 1 mg) were dissolved in DMSO. Diagnostic resonances and peak patterns confirmed the presence of all indicated residues. Electro-spray mass spectroscopy confirmed the appropriate molecular weights.

Opioid receptor binding assays

All newly synthesized deltorphin analogues were assayed for binding to μ [versus [³H]DAMGO], or

[³H](D-Ala², N-MePhe⁴, Gly⁵-ol)enkephalin), to δ (versus [³H]DPDPE, or [³H](D-Pen², D-Pen⁵)enkephalin], and to κ (versus [³H]U69,593, or 5a,7a,8b-(–)-N-[7-(1-pyrrolidinyl)-1-oxaspiro(4,5)dec-8-yl]benzeneacetamide] opioid receptors.

Receptor binding assays measured displacement by the test compounds of radiolabelled receptor-selective ligands from guinea pig brain homogenates, using 1.2 nM [³H]DAMGO for the μ receptor, 2.5 nM [³H]DPDPE for the δ receptor and 1.0 nM [³H]U69,593 for the κ receptor, as described previously.³⁵ IC₅₀ values were obtained by linear regression from plots relating inhibition of specific binding to the log of 12 different ligand concentrations, using the RADLIG computer software program (Biosoft Software)³⁶ For binding to κ receptors, which was expected to be weak, the protocol was altered to include only five ligand concentrations and was performed in duplicate; these values are not reported since there was no substantial κ receptor binding. K_i values were calculated using values for K_D of each ligand. Each K_i value reported is the mean of two to four determinations, each performed in triplicate.

Calculation of isolated side-chain properties

QSAR properties were calculated for the isolated side chains cleaved at the α -carbon and capped with a hydrogen atom. Values are calculated using the Chem-Plus utility of the HyperChem v. 4 and 5 software package (HyperCube, Inc.). Calculations of log P and polarizability employ the methods of Viswanadhan et al.³⁷ and Miller,³⁸ respectively. Those calculations are not dependent on structure optimization. Calculation of van der Waals surface area and volume employs the grid method of Bodor et al.³⁹ based on the atomic radii of Gavezzotti,⁴⁰ and is weakly dependent on the three-dimensional structure. For this purpose, the structures of the isolated side chains were optimized using HyperChem's MM+ implementation of Allinger's MM2 molecular mechanics force field.⁴¹ Various other derived properties are calculated as previously described.³² Briefly, the equivalent box dimensions of width, thickness (smallest dimension), and length (largest dimension) were determined using HyperChem's periodic box facility to fit the structure to the smallest possible rectangular box. The normal, defined as the maximum distance the side chain can extend from the backbone, was measured as the through-space distance from the β -carbon to the most distant atom of the side chain in the MM+ optimized structure. Ovality³⁹ is the ratio of surface area to the surface area of a sphere of the same volume, and increases from unity for either stretching (prolate) or squashing (oblate) distortions from spherical. Although intended to allow isolation of shape from size, in our experience it serves as a length-weighted measure of size.³² The steric factor is the product of the van der Waals surface area and the square of the diameter of the equivalent sphere. This quantity was discovered to provide the best multiple-regression steric repulsion term when the binding pocket model was applied to the positions 3 and 4 analogues.³² Finally, a β crowding variable was defined by the following simple

scale: the sum of 1 for each non-H group attached to the β -carbon, plus 1/2 for each non-H group attached to each sp³ γ -carbon. For example, Ala, 0; Phe, 1; Nva, 1.5; Val, 2; Ile, 2.5; Tle, 3.

Langevin dynamics of peptide fragments

Five hundred picosecond (ps) Langevin dynamics runs were performed by HyperChem, starting from the PM3 optimized structure. A single 500 ps dynamics run required between 4 and 12 days of computer time (Dell Dimension XPS 300 MHz Pentium II). Run conditions included a constant temperature of 310 K, temperature bath relaxation constant of 0.1 ps, a dynamics step size of 0.5 fs, and a frictional coefficient of 41 ps^{–1}. The latter was calculated for the Valine peptide fragment (M_r , 172) assuming an average effective radius of 7 Å in water of viscosity 0.89 centipoise. The instantaneous values of the four primary geometrical variables were recorded every 0.1 ps, creating a data file of 5000 points per variable per run, which can be analyzed in a spreadsheet program. The phi and psi data must be corrected to give continuous angle ranges because when the generally-negative phi or generally-positive psi angles exceed 180° in magnitude, HyperChem 'wraps' them to values of the opposite sign. Wrapped values were corrected by subtracting or adding 360° to create angles less than –180° (phi) or greater than +180° (psi). Derived variables consisting of the sum, psi + phi, and the difference, psi – phi, were also investigated.

Data analysis

Data analysis began with screening of all variables using the Explore utility of the SPSS® v. 8.0 statistics package, including various tests of normality and the box plot analysis for outliers and extremes. Subsequent correlation and regression analyses were performed using the Microsoft® Excel 97 spreadsheet program and SPSS® v. 8.0. Separate QSAR analyses were performed for the δ and μ data subsets within each of the residue 5 and residue 6 analogue sets. In addition to the hypothesis-driven regression analyses for the size-related predictors, complete bivariate correlation and stepwise multiple regression analyses were performed to discover any unanticipated relationships that might exist.

All analyses reported were preceded by deletion of data designated as univariate extreme outliers by the SPSS box plot procedure. In order to retain as much information as possible, missing data were accommodated by pairwise deletion in the correlation and regression analyses. Also, to retain the position 5 data that exceeded the binding assay limits, the $K_{i\mu}$ and 10 μ M-limit percentage data were combined as a rank-ordered sequence. This also allowed retention of the extreme outlier, 2-Nal. The price for this adjustment is loss of distribution normality and associated probability information (i.e., p values are unreliable). Following each regression run, residual plots and related diagnostics provided by SPSS® were carefully scrutinized to assure that only legitimate relationships were retained.⁴²

Acknowledgements

Opioid receptor binding assays were graciously performed under the direction of Dr. Henry I. Mosberg at the University of Michigan. Electrospray mass spectral analyses were provided by Dr. Phil Andrews and colleagues at The University of Michigan Protein and Carbohydrate Structure Facility. Funding for this research has been provided by the Eastern Michigan University Chemistry Department, an EMU Graduate School Support Award (D.L.H.), an EMU Faculty Research Fellowship (D.L.H.), a Josephine Nevins Keal Professional Development Award for Women Faculty (D.L.H.) and primarily by a Bristol-Myers Squibb Award of Research Corporation (D.L.H.).

References and Notes

- Lord, J. A. H.; Waterfield, J. A.; Hughes, J.; Kosterlitz, H. W. *Nature* **1977**, *267*, 495.
- Erspermer, V. *Int. J. Dev. Neuro.* **1992**, *10*, 3.
- Fukuda, K.; Kato, S.; Mori, K. *J. Biol. Chem.* **1995**, *270*, 6702.
- Mosberg, H. I. *Biopolymers (Pept. Sci.)* **1999**, *51*, 426.
- Law, P. Y.; Wong, Y. H.; Loh, H. H. *Biopolymers (Pept. Sci.)* **1999**, *51*, 440.
- Schiller, P. W.; Weltrowska, G.; Berezowska, I.; Nguyen, T. M.-D.; Wilkes, B. C.; Lemieux, C.; Chung, N. N. *Biopolymers (Pept. Sci.)* **1999**, *51*, 411.
- Schiller, P. W.; Nguyen, T. M.-D.; Weltrowska, G.; Wilkes, B. C.; Marsden, B. J.; Lemieux, C.; Chung, N. N. *Proc. Natl. Acad. Sci. U.S.A.* **1992**, *89*, 11871.
- Schiller, P. W.; Weltrowska, G.; Schmidt, R.; Nguyen, T. M.-D.; Berezowska, I.; Lemieux, C.; Chung, N. N.; Carpenter, K. A.; Wilkes, B. C. *Analgesia* **1995**, *1*, 703.
- Schiller, P. W.; Fundytus, M. E.; Merovitz, L.; Weltrowska, G.; Nguyen, T. M. D.; Lemieux, C.; Chung, N. N.; Coderre, T. J. *J. Med. Chem.* **1999**, *42*, 3520.
- Abdelhamid, E. E.; Sultana, M.; Portoghese, P. W.; Takemori, A. E. *J. Pharmacol. Exp. Ther.* **1991**, *258*, 299.
- Fundytus, M. E.; Schiller, P. W.; Shapiro, M.; Weltrowska, G.; Coderre, T. *Eur. J. Pharmacol.* **1995**, *286*, 105.
- Hepburn, M. J.; Little, P. J.; Gingras, J.; Kuhn, C. M. *J. Pharmacol. Exp. Ther.* **1997**, *281*, 1350.
- Zhu, Y.; King, M. A.; Schuller, A. G. P.; Nitsche, J. F.; Reidl, M.; Elde, R. P.; Unterwald, E.; Pasternack, G. W.; Pintar, J. E. *Neuron* **1999**, *24*, 243.
- Erspermer, V.; Melchiorri, P.; Falconieri-Erspermer, G.; Negri, L.; Corsi, R.; Severini, C.; Barra, D.; Simmaco, M.; Kreil, G. *Proc. Natl. Acad. Sci. U.S.A.* **1989**, *86*, 5188.
- Salvadori, S.; Marastoni, M.; Balboni, G. *J. Med. Chem.* **1991**, *34*, 1656.
- Lazarus, L. H.; Salvadori, S.; Attila, M.; Grieco, P.; Bundy, D. M.; Wilson, W. E.; Tomatis, R. *Peptides* **1993**, *14*, 21.
- Sagan, S.; Charpentier, S.; Delfour, A.; Amiche, M.; Nicolas, P. *Biochem. Biophys. Res. Commun.* **1992**, *187*, 1203.
- Mosberg, H. I.; Kroona, H. B.; Omnaas, J. R.; Scobczyk-Kojiro, K.; Bush, P.; Mousigian, C. In *Peptides: Chemistry, Structure and Biology, Proc. Am. Pept. Symp.*, 13th meeting date; Hodges, R. S., Smith, J. A., Eds.; ESCOM: Leiden, 1993; p 514.
- Lazarus, L. H.; Salvadori, S.; Tomatis, R.; Wilson, W. E. In *Peptides: Chemistry and Biology*; 12th American Peptide Symposium; Smith, J. A.; Rivier, J. E., Eds.; Cambridge: New York, 1991; p 144.
- Balboni, G.; Marastoni, M.; Picone, D.; Salvadori, S.; Tancredi, T.; Tesmussi, P.; Tomatis, R. *Biochem. Biophys. Res. Commun.* **1990**, *169*, 617.
- Segawa, M.; Ohno, Y.; Dot, M.; Inoue, M.; Ishida, I.; Iwashita, T. *Int. J. Pept. Prot. Res.* **1994**, *44*, 295.
- Tourwe, D.; Verschuere, K.; Frycia, A.; Davis, P.; Porreca, F.; Hruby, V.; Toth, G.; Jaspers, H.; Verheyden, P.; van Binst, G. *Biopolymers* **1996**, *38*, 1.
- Nikiforovich, G.; Hruby, V. *Biochem. Biophys. Res. Commun.* **1990**, *173*, 521.
- Nikiforovich, G.; Prakash, O.; Gehrig, C.; Hruby, V. *J. Am. Chem. Soc.* **1993**, *115*, 3399.
- Crescenzi, O.; Amodeo, P.; Cavicchioni, G.; Guerrini, R.; Picone, D.; Salvadori, S.; Tancredi, T.; Temussi, P. A. *J. Pept. Sci.* **1996**, *2*, 290.
- Misicka, A.; Lipkowski, A. W.; Horvath, R.; Davis, P.; Kramer, T. H. *Life Sci.* **1992**, *51*, 1025.
- Sasaki, Y.; Ambo, A.; Suzuki, K. *Biochem. Biophys. Res. Commun.* **1991**, *180*, 822.
- Crescenzi, O.; Amodeo, P.; Cavicchioni, G.; Guerrini, R.; Picone, D.; Salvadori, S.; Tancredi, T.; Tesmussi, P. *J. Pept. Sci.* **1996**, *2*, 290.
- Naim, M.; Nicolas, P.; Benajiba, A.; Baron, D. *J. Pept. Res.* **1998**, *52*, 443.
- Lazarus, L. H.; Bryant, S. D.; Cooper, P. S.; Salvadori, S. *Prog. Neurobiol.* **1999**, *57*, 377.
- Heyl, D. L.; Schullery, S. E. *Curr. Med. Chem.* **1997**, *4*, 117.
- Schullery, S.; Mohammedshah, T.; Makhlof, H.; Marks, E.; Wilenkin, B.; Escobar, S.; Mousigian, C.; Heyl, D. *Bioorg. Med. Chem.* **1997**, *5*, 2221.
- Heyl, D.; Sanvordekar, M.; Dogruyol, G.; Salamoun, M.; Rodgers, D.; Renganathan, K.; Mousigian, C.; Schullery, S. *Prot. Pept. Lett.* **1999**, *6*, 359.
- HyperChem[®]. *Computational Chemistry*. HyperCube: Waterloo, Ontario, 1996.
- Mosberg, H. I.; Heyl, D. L.; Omnaas, J. R.; Haaseth, R. C.; Medzihradsky, F.; Smith, C. B. *Mol. Pharmacol.* **1990**, *38*, 924.
- Munson, P. J.; Rodbard, D. *Anal. Biochem.* **1980**, *107*, 220.
- Viswanadhan, V. N.; Ghose, A. K.; Revankar, G. N.; Robins, R. K. *J. Chem. Inf. Comput. Sci.* **1989**, *29*, 163.
- Miller, K. J. *J. Am. Chem. Soc.* **1990**, *112*, 8533.
- Bodor, N.; Gabanyi, Z.; Wong, C. *J. Am. Chem. Soc.* **1989**, *111*, 3783.
- Gavezotti, A. *J. Am. Chem. Soc.* **1983**, *105*, 5220.
- Allinger, N. A. *J. Am. Chem. Soc.* **1977**, *99*, 8127.
- Tabachnik, B. G.; Fidell, L. S. In *Using Multivariate Statistics*, 3rd ed.; HarperCollins: New York, 1996.